Comparison between *Apicystis cryptica* sp. n. and *Apicystis bombi* (Arthrogregarida, Apicomplexa): Gregarine parasites that cause fat body hypertrophism in bees

Karel Schoonvaere[a], Marleen Brunain[a], Femke Baeke[b,c], Michiel De Bruyne[b,c], Riet De Rycke[b,c], Dirk C. de Graaf[a,*]

[a]*Laboratory of Molecular Entomology and Bee Pathology, Department of Biochemistry and Microbiology, Faculty of Sciences, Ghent University, Krijgslaan 281 Block S2, 9000 Ghent, Belgium*
[b]*Department for Biomedical Molecular Biology, Ghent University, VIB Center for Inflammation Research, Ghent, Belgium*
[c]*Ghent University Expertise Centre for Transmission Electron Microscopy and VIB BioImaging Core, Ghent, Belgium*

Abstract

The molecular divergence, morphology and pathology of a cryptic gregarine that is related to the bee parasite *Apicystis bombi* Lipa and Triggiani, 1996 is described. The 18S ribosomal DNA gene sequence of the new gregarine was equally dissimilar to that of *A. bombi* and the closest related genus *Mattesia* Naville, 1930, although phylogenetic analysis supported a closer relation to *A. bombi*. Pronounced divergence with *A. bombi* was found in the ITS1 sequence (69.6% similarity) and seven protein-coding genes (nucleotide 78.05% and protein 90.2% similarity). The new gregarine was isolated from a *Bombus pascuorum* Scopoli, 1763 female and caused heavy hypertrophism of the fat body tissue in its host. In addition, infected cells of the hypopharyngeal gland tissue, an important excretory organ of the host, were observed. Mature oocysts were navicular in shape and contained four sporozoites, similar to *A. bombi* oocysts. Given these characteristics, we proposed the name *Apicystis cryptica* sp. n. Detections so far indicated that distribution and host species occupation of *Apicystis* spp. overlap at least in Europe, and that historical detections could not discriminate between them. Specific molecular assays were developed that can be implemented in future pathogen screens that aim to discriminate *Apicystis* spp. in bees.

Introduction

Protozoans of the order Arthrogregarida (phylum Apicomplexa) are parasites of arthropods (Cavalier-Smith 2014). Five species have been associated with pathologies in bees (Hymenoptera; Anthophila clade), of which four septate gregarines described from the honey bee *Apis mellifera* Linnaeus, 1758 (Stejskal 1965) and a single aseptate gregarine, also referred to as a neogregarine, described from multiple bumble bee species in Canada (Liu et al. 1974). Upon its discovery, the latter gregarine was named *Mattesia bombi* and two decades later it was accommodated in the new genus *Apicystis* Lipa and Triggiani after its re-discovery in Europe (Lipa and Triggiani 1992, 1996). *Apicystis* was differentiated from *Mattesia* by the navicular instead of the lemon-shaped

---

*Corresponding author.
  E-mail address: Dirk.deGraaf@UGent.be (D.C. de Graaf).

oocysts, the presence of four instead of eight sporozoites per oocyst and specialization of bee hosts. Although bumble bees are considered to serve as the predominant hosts (Macfarlane et al. 1995), *A. bombi* has also been detected in honey bees (Menail et al. 2016; Plischuk et al. 2011; Schulz et al. 2019), stingless bees (Nunes-Silva et al. 2016) and solitary wild bees (Ravoet et al. 2014; Tian et al. 2018) but no insect hosts other than bees so far. Early monitoring studies assumed a cosmopolitan distribution of *Apicystis* (Lipa and Triggiani 1996). However, the more recent detections of *A. bombi* in South-America (Plischuk and Lange 2009) and Asia (Morimoto et al. 2013) have raised questions about its true native range (Maharramov et al. 2013; Meeus et al. 2011). The prevalence of *A. bombi* differs greatly across studies and castes (queens, workers and males) with average reports of 5–10% in 5 bumble bees, 10–15% in honey bees and invasive bumble bees (Jones and Brown 2014; Plischuk et al. 2011, 2017) and over 25% in populations proximous to commercial pollinator customers (Graystock et al. 2014).

Gregarines classified in the former order Neogregarinorida are notably more virulent than other parasites (Undeen and Vávra 1997). Infections are generally limited to a specific tissue, often the fat body or Malpighian tubules (Yaman and Radek 2017) resulting in proliferation and destruction of the infected tissue. The life cycle of these parasites is complex and that of *A. bombi* is moderately resolved thanks to a single ultrastructure study (Liu et al. 1974). Infection starts with the oral uptake of a viable oocyst (cfr. long-living spore) and release of four sporozoites in the midgut lumen. The sporozoites penetrate the midgut wall and undergo asexual and sexual reproduction in the fat body cells. Prior to sporogony, the gametocyst contains two oval sporoblasts that quickly develop into young oocysts (Valigurová and Koudela 2006). As they mature, the oocyst wall thickens, a pair of polar plugs at the ends of the oocysts become visible and the gametocyst membranes ultimately dissociates. The cycle is repeated in the same host by autoinfection of fat body cells. Typically, healthy fat body cells appear yellow while heavily infected cells appear swollen and distinctly white as a result of hypertrophism (Lipa and Triggiani 1996). Other than the fat body, oocysts have been detected in the midgut and hindgut body parts of bees and in a single case in the spermatheca of a mated bumble bee queen (Liu et al. 1974). The exact transmission route of *A. bombi* has not been studied in detail except for Graystock et al. (2015) demonstrating horizontal transmission via contaminated flowers. In other studies, transmission via the oral-fecal route and ingestion of contaminated food sources or dead bodies in the nest are assumed (Jones and Brown 2014; Schmid-Hempel 1998). The exact mechanism by which mature oocysts re-enter the alimentary tract is unknown to date. Experimental studies have demonstrated a negative effect of *A. bombi* infection on bee longevity (Graystock et al. 2016; Jones and Brown 2014; Tian et al. 2018) and colony foundation success in bumble bee queens (Jones and Brown 2014; Rutrecht and Brown 2008).

Microscopic examination for the presence of navicular oocysts has been an approachable method for *A. bombi* detection. More recently, molecular techniques have gained popularity as they are more scalable and versatile (Meeus et al. 2010). In metagenomic studies, the parasite's subset genetic material (subtranscriptome) is identified along that of the host and other inhabitants. In a previous metagenomic study, we discovered a gregarine in the bumble bee *Bombus pascuorum* that showed considerable DNA sequence dissimilarity (molecular divergence) with respect to *A. bombi* (Schoonvaere et al. 2018). In a follow-up study, we aimed at re-sampling the parasite for microscopic analysis and investigated its pathology, morphology and genetic background. Here, we report our findings that two similar species infect bumble bees. We propose to retain the name *Apicystis bombi* for the species that matches the majority of historical reports, whereas the name *Apicystis cryptica* sp. n. is proposed for the species recently discovered by a metagenomic survey.

Materials and methods

Sample collection

Specimens of the genus *Bombus* were collected during two independent sampling rounds, the first in 2015 and the second in 2017, in Belgium. The first sampling round was carried out at five localities as part of metagenomic studies in wild bees (Schoonvaere et al. 2016, 2018). All sampling events were carried out during the months April and May on rainless days with favorable temperature higher than 17 °C. Sampling permissions in the southern provinces were granted by Ref. Avenant 3 déro 2014/RS/n°18. Following net trapping, bees were directly stored on carboglass and later transferred to −80 °C in the lab. In the first locality, one out of five collected *B. pascuorum* queens was infected with *A. cryptica* sp. n. (sample name A06, date of sampling 14.IV.2015; Trivières; decimal degree coordinates 50.45316, 4.134969). In the second locality, also one out of five collected *B. pascuorum* queens was infected with *A. cryptica* sp. n. (A88, 21.IV.2015; Torgny; 49.511117, 5.482273). In the third locality, two out of five collected *Bombus terrestris* Linnaeus, 1758 queens were infected with *A. bombi* (A50; 17.IV.2015; Ghent; 51.024801, 3.711731 and A96; 04.V.2015; Ghent; 51.023306, 3.709452). Out of 10 sampled bumble bee specimens in each of the two other localities, no gregarine infections were found (Moorsel and Francorchamps). Host species identification was done by barcoding as described by Schoonvaere et al. (2018). The second sampling round was carried out for microscopy purposes. Here, we focused on the species *B. pascuorum* because both *A. bombi* and *A. cryptica* sp. n. have been found in this bumble bee species in Belgium (Schoonvaere et al. 2018). Moreover, we aimed to collect foraging *B. pascuorum* (females) in mid-June to ensure a high gregarine infection load, being either infected workers or late queens that failed in colony founding. Bees were captured, euthanized and processed on

Table 1. PCR primer sequences used in this study.

Name	Sequence (5′ > 3′)	Specific?	Reference
ApBF1[a]	CGTACTGCCCTGAATACTCCAG	No	Meeus et al. (2010)
ApBR1	TGAAAGCGGCGTATACATGA	No	Meeus et al. (2010)
ApB143r	TGCCACTTTTCTTTGCAGTC	No	This study
ApB170f	CTTCGGTATAGTTAATTGGTGATCCA	Yes	This study
ApB681r	CACCTCTAACATTTTATTTTAGCAAGC	Yes	This study
ApC500f[b]	CAACCCCATGCAAGTATCAA	No	This study
ApC666r	TGCCAATAAAAACAAAGCTCAA	Yes	This study
ApUF2[c]	ATCTGGTTGATCCTGCCAGT	No	Meeus et al. (2010)
ApUR2	TTTCTCATTCTTCAGATGATTTGG	No	Meeus et al. (2010)

[a] ApB, *Apicystis bombi*.
[b] ApC, *Apicystis cryptica* sp. n.
[c] ApU, universal for genus *Apicystis*.

the same day without a freeze-thaw cycle. This procedure allowed us to sample up to eight bees per day. The location was Moorsel (50.953475, 4.108034 ± 100 m). Eight specimens B01-08 were collected and processed on 10.VI.2017 and five more specimens B09-13 on 15.VI.2017. Specimens used for microscopy were B04 (healthy control), B05, B06, B10 and B13.

DNA extraction

DNA extractions from fresh material were done by the chelex-proteinase K method starting from a bee hind leg as described by Schoonvaere et al. (2018). DNA extraction from tissues dissected in fixation buffer (4% formaldehyde, 2.5% glyceraldehyde, 0.1 M cacodylate buffer) was done using a modified phenol-chloroform-isoamyl alcohol (PCI) protocol. Dissection time never exceeded 30 min. Fixed tissues were washed in phosphate buffered saline three times. Samples were homogenized by beat-beating in 0.5 ml phosphate buffered saline and approximately 70 μl zirconium beads and five steel beads using a Precellys instrument. One volume of PCI was added to the homogenate, vortexed and centrifuged for 5 min, max speed at room temperature. The upper aqueous phase was isolated and 1/10 volume 3 M sodium acetate pH 5.2 was added. Two volumes ice-cold absolute ethanol were added, gently mixed and samples were incubated for 2 h at −20 °C. After incubation, precipitated DNA was centrifuged for 30 min at 4 °C, max speed and the (invisible) pellet was washed with 70% ethanol. All supernatant ethanol was removed and the pellet was allowed to air-dry for 15 min. Finally, DNA was re-suspended in 30 μl 100 mM Tris−HCl buffer pH 8 preheated to 60 °C.

Molecular detection

The 18S ribosomal DNA (rDNA) gene was sequenced based on the method described by Meeus et al. (2010). Briefly, primers used for the overlap amplification were forward/reversed ApUF2/ApBR1 (NeoL) and ApBF1/ApUR2

(NeoR). PCR reaction conditions were the same, with the exception of a proofreading enzyme (Platinum Pfx, Life Technologies). PCR products were submitted to GATC Biotech AG (Constance, Germany) for dideoxy DNA sequencing in both directions. Sequence trace files of NeoL and NeoR products were examined and assembled using SeqTrace (Stucky 2012), the resultant sequence was GenBank record MF998086.1. Sequence integrity was confirmed by BLAST analysis using MF998086.1 as a query against the Sequence Read Archive records SRR6148372 and SRR6148369. Sequence alignment was done using MUSCLE (default options) embedded in the EBI multiple sequence alignment tools portal. Variable sequence regions were used as a template for specific primer design using the online primer3 tool (Untergasser et al. 2012). Specific and historical primer sequences used in *Apicystis* molecular detection are included in Table 1. The PCR reactions contained final concentrations 1 mM $MgCl_2$, 0.2 mM dNTPs, 2 μM of each primer, 1 unit HotStarTaq Plus DNA polymerase (Qiagen, 203605 in ddH_2O and colored 10x buffer. We used 1 μl of template DNA sample (see section DNA extraction). The PCR reaction conditions were 5 min at 95 °C, 35 cycles of 30 s at 94 °C, 30 s at 55 °C and 45 s at 72 °C, and a final elongation step of 10 min at 72 °C.

Bioinformatics

BLASTn analysis was used against the latest non-redundant (nt), Transcriptome Shotgun Assembly (TSA) or Sequence Read Archive databases. Protein-coding genes were selected after metagenomics profiling described by Schoonvaere et al. (2018). For seven genes we obtained high-coverage assembly. These were preferred over low-expressed genes because coverage correlates with assembly accuracy and completeness. Full and abbreviated gene names: heat-shock protein 70 (hsp70), heat-shock protein 90 (hsp90), elongation factor 1 alpha (ef1a), fibrillarin (fib), methionine adenosyltransferase (mat), ribosomal protein S6 (rps6), tubuline beta-chain (tubb). Conservation in the phylum Apicomplexa was verified by (t)BLASTn/x analysis and we

confirmed assembly correctness by mapping the original NGS reads to the transcripts (*A. bombi*: SRR6148372 and SRR6148369; *A. cryptica* sp. n.: SRR1502945).

Phylogenetic analyses

We followed the revised classification by Cavalier-Smith (2014) with respect to gregarines. In this classification, gregarines of the former order Neogregarinorida were demonstrated to be multiply polyphyletic and all neogregarine species are accommodated in the broader order Arthrogregarida. Despite of our awareness that a former classification is still commonly used, we favor the revised classification because it adds molecular divergence evidence to former systematic criteria (species morphology, life cycle and host occupancy). The 18S rDNA locus was used as a phylogenetic marker because it is the most widely available DNA sequence for arthrogregarines in public repositories. Arthrogregarine species of the families Ophryocystidae, Lipotrophidae, Monocystidae, Syncystidae and Gregarinidae were included in the phylogenetic analysis. Species of Cryptosporidiidae (order Cryptogregarida) were used as an outgroup. Fasta sequences were retrieved from GenBank and aligned by MUSCLE (default options) in MEGA X (Kumar et al. 2018) using the MUSCLE algorithm at default parameters. The optimal nucleotide substitution model was determined as Tamura 3-parameter model (Tamura 1992) and the evolutionary relation was inferred using the Maximum Likelihood method. The initial tree topology was obtained automatically (Neighbor-Join and BioNJ algorithms) using the Maximum Composite Likelihood approach. A discrete Gamma distribution was used (+G, 4 categories) and gaps or missing data were omitted (complete deletion option). Confidence levels were calculated by applying the bootstrap method and 1000 replicates.

Light microscopy and oocyst measurements

Mature oocysts were distinguished from immature oocysts by (i) the dissociation of the gametocyst membrane (= unpaired oocysts) and (ii) the presence of two dense polar plugs at the front and rear sides. Mature oocysts may also be distinguished by the more refractive surface (appearing more bright) than immature oocysts. The samples used for mature oocyst measurements originated from the -80 °C stored mesosoma homogenate of samples A88, A50 and A96 (see Sample Collection). Length and width of spores were measured using an internal calibrator on a Leica DMLS instrument at $400\times$ magnification. Photographs were taken using a Zeiss AxioCam ERC 5 s camera. Oocyst sizes are reported as mean $\pm$ standard error. Statistical two-sample t-tests were performed in R v3.4.2 (R Core Team 2017).

Transmission electron microscopy

Bees were not frozen or kept alive for longer than 6 h between capture and dissection. Prior to dissection, the bee was euthanized by decapitation. The prosoma, mesosoma and metasoma were cut open using a sterile pair of scissors in a 1 ml droplet of fixation buffer (4% formaldehyde, 2.5% glutaraldehyde, 0.1 M cacodylate buffer). Quickly, six tissue types were isolated using sterilized forceps: hypopharyngeal gland (HG) tissue from the prosoma, flight muscle (MU) tissue from the mesosoma and the alimentary tract (ALI), fat body (FB), malpighian tubules (MT) and ovaries (OV) from the metasoma. The dissection took no longer than 15 min per bee and the immersion of internal organs in fixation buffer was ensured during the entire procedure. Individual tissues were transferred to a separate, sealed mesh container. The remaining tissue was used for nucleic acid extraction (see DNA extraction). Samples were immersed in fresh fixation buffer, placed in a vacuum oven for 30 min and left rotating for 3 h at room temperature and subsequently rotating over night at 4 °C. After washing, samples were postfixed in 1% OsO_4 with $K_3Fe(CN)_6$ in 0.1 M cacodylate buffer, pH 7.2. After washing in ddH_2O, samples were dehydrated through a graded ethanol series, including a bulk staining with 2% uranyl acetate at the 50% ethanol step followed by embedding in Spurr's resin. To select the area of interest on the block and in order to have a larger overview of the phenotype, semithin sections were first cut at 0.5 μm and stained with toluidin blue. Ultrathin sections of a gold interference color were cut using an ultra-microtome (Leica EM UC6), followed by a post-staining in a Leica EM AC20 for 40 min in uranyl acetate at 20 °C and for 10 min in lead stain at 20 °C. Sections were collected on Formvar-coated copper slot grids. Grids were viewed with a JEM 1400plus transmission electron microscope (JEOL, Tokyo, Japan) operating at 60 kV.

Results

Molecular discrimination of *A. bombi* and *A. cryptica* sp. n

Pairwise comparison of *A. bombi* and *A. cryptica* sp. n. 18S rDNA gene sequences revealed only two variable regions with considerable sequence dissimilarity (Fig. 1a, b). All historical PCR primers developed for "*Apicystis bombi*" diagnosis fell outside these regions. We used the variable regions as a template for specific primer design. For *A. bombi*, two primer sets had to be developed before a specific assay was obtained. The first set (ApUF2/ApB143r) was not specific despite a 2-nt gap difference in the reverse primer sequence. A second primer set (ApB170f/ApB681r) specifically amplified a 512 bp sequence (Fig. 1c). For *A. cryptica* sp. n., primers ApC500f/ApI666r specifically amplified a 167 bp
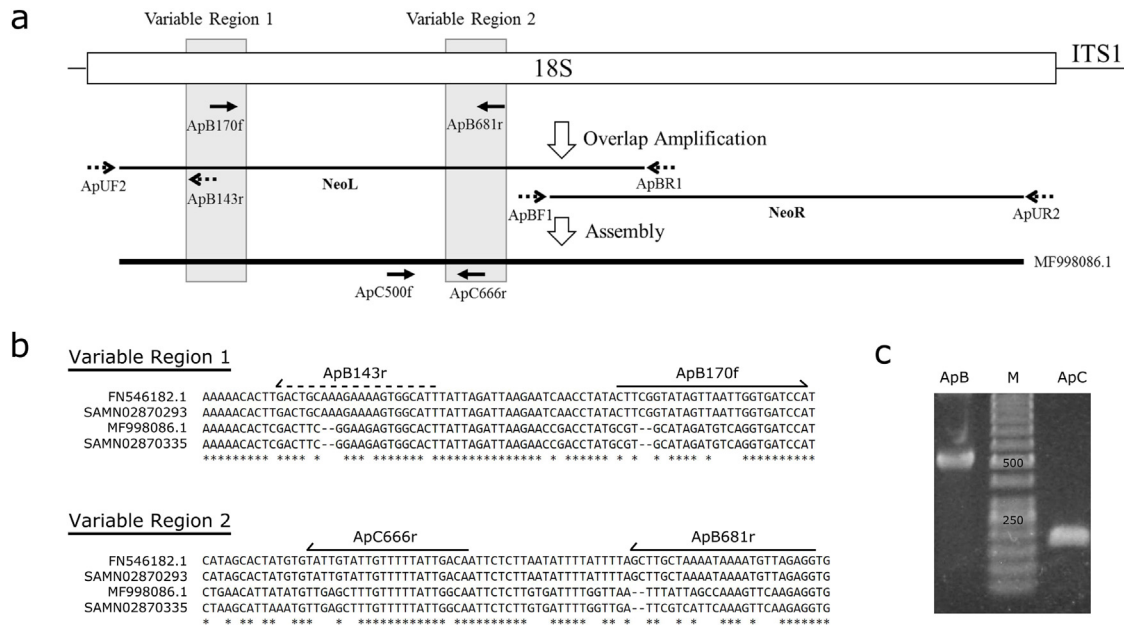
Fig. 1. a–c. Molecular discrimination of *Apicystis bombi* and *Apicystis cryptica* sp. n. **a)** Overlap amplification of *A. cryptica* sp. n. 18S ribosomal DNA gene sequence using (Meeus et al., 2010) PCR primers ApUF2/ApBR1 (NeoL) and ApBF1/ApUR2 (NeoR) followed by assembly into GenBank accession MF998086. PCR primers are indicated by arrows, either species specific primers (full line) or non-specific primers (dashed lines). Primer sequences are included in Table 1. **b)** Multiple sequence alignment of variable regions 1 and 2 of all *Apicystis* spp. records that were sequenced to date. FN546182, SAMN02870293 = *A. bombi*; MF998086 = *A. cryptica* sp. n.; SAMN02870335 = undescribed species of *Megachile willughbiella*. Specific (full line) and non-specific (dashed line) primer binding sites are illustrated on top of the alignment. **c)** Gel-electrophoresis of specific PCR assay results for *A. bombi* (ApB170f/ApB681r, first lane) and *A. cryptica* sp. n. (ApC500f/ApC666r, third lane) infected bumble bees. *Apicystis bombi* specific PCR generates a 512 bp amplicon, *A. cryptica* sp. n. specific PCR generates a 167 bp amplicon. Second lane M = GeneRuler 50 bp DNA ladder (Thermo Scientific).

sequence (Fig. 1c). The specific assays were used throughout the study to successfully differentiate *A. bombi* from *A. cryptica* sp. n. Of the 13 *B. pascuorum* females collected in the second sampling round, one tested positive for *A. bombi* (B06) and three tested positive for *A. cryptica* sp. n. (B05, B10, B13). Double infections were not detected.

Divergence based on 18S, ITS1 and protein-coding genes

Phylogenetic analysis based on the 18S rDNA gene separated *A. cryptica* sp. n. from *A. bombi* despite a low (52%) bootstrap support (Fig. 2). Both genotypes were separated from the genus *Mattesia* as a sister group with 84% bootstrap support. In the phylogenetic analysis, also three 18S rDNA gene sequences of gregarines were included that were discovered by tBLASTn against public TSA datasets: *A. bombi* in BioSample SAMN02870293 (*Eucera nigriscens*, Apidae), *Apicystis* sp. that is more related to *A. cryptica* sp. n. than to *A. bombi* in SAMN02870335 (*Megachile willughbiella*, Megachilidae) and a far-branching *Gregarina* sp. most related to *G. diabrotica* in SAMN02870316 (*Hylaeus variegatus*, Colletidae). GenBank and TSA accession numbers are summarized in Supplemental information 1. Divergence

between *A. bombi* and *A. cryptica* sp. n. was more elaborate in the ribosomal ITS1 sequence. The ITS1 part was highly dissimilar and caused a 370 bp sequence of the 18S- ITS1-5.8S to misalign by default BLAST parameters. Alignment was successful after applying minimal gap costs (Existence: 2, Extension: 2). Over the entire query length, *A. bombi* and *A. cryptica* sp. n. had 69% nucleotide identity. Phylogenetic analysis based on this region of all available GenBank and TSA records resulted in a clear bifurcation between the species (Supplemental Fig. 1). The TSA records of *A. cryptica* sp. n. GHFQ01001441.1 (sample A06) and GHFY01001509.1 (sample A88) clustered with six GenBank records isolated from bumble bees in West-Siberia (KY126621, KY126622, KY126625, KY126628, KY126631 and KY126632). Of the 120 GenBank records referred to as *A. bombi* to date, 107 truly belong to *A. bombi*, 12 belong to *A. cryptica* sp. n. and 1 Mexican record is ambiguous. Unambiguous *A. bombi* identifications originate from Eurasia (Ireland, Japan and West-Siberia) and South-America (Argentina, Brazil, Colombia and Mexico) whereas unambiguous *A. cryptica* sp. n. identifications are currently limited to Belgium and West-Siberia (Supplemental information 1). Next to ribosomal loci, seven protein-coding genes with relative high expression were compared (Table 2). Sequence records originate from the parasite subtranscrip-
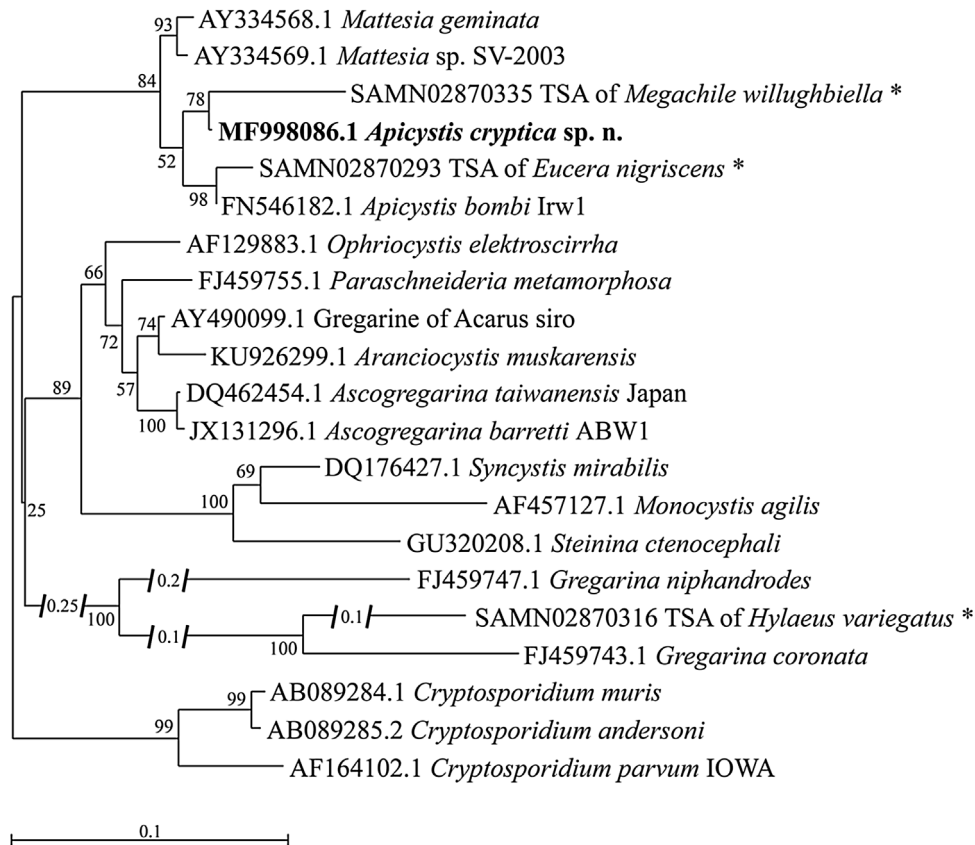
Fig. 2. Phylogenetic analysis of *Apicystis bombi* and *Apicystis cryptica* sp. n. based on 18S ribosomal DNA gene. The tree topology with the highest log likelihood (−5443.83) is shown. A total of 921 positions were included in the final dataset. Bootstrap support values (n = 1000) are indicated in percentages. The scale bar denotes the number of substitutions per site. *Apicystis bombi* is clustered together with *A. cryptica* sp. n. (52 support) and both are separated from *Mattesia* spp. (84 support). BioSample records of bee species of which the public Transcriptome Shotgun Assembly (TSA) dataset contains gregarine sequences are indicated by an asterisk. The gregarine of *Eucera nigriscens* is most likely *A. bombi*, the gregarine of *Megachile willughbiella* is most related to *A. cryptica* sp. n. and the gregarine of *Hylaeus variegatus* is most related to *Gregarina coronata*, a septate gregarine described from beetles.

Table 2. BLAST identity between *Apicystis* spp. of ribosomal and protein-coding genes.

Gene	*A. bombi*	*A. cryptica* sp. n.	Nucleotide %	Protein %
18S rDNA	FN546182.1	MF998086.1	95,36	–
ITS1[a]	KY126621.1	KY126623.1	69,57	–
hsp70	GBPG01002195.1	GHFY01000033.1	78,81	94,63
hsp90	GBPG01002200.1	GHFY01000029.1	77,43	86,78
ef1a	GBPG01026098.1	GHFY01011377.1	82,68	96,5
fib	GBPG01025281.1	GHFY01015325.1	78,28	92,95
mat	GBPG01025316.1	GHFY01014334.1	74,76	83,16
rps6	GBPG01023297.1	GHFY01007309.1	74,37	81,25
tubb	GBPG01000440.1	GHFY01003556.1	80,05	96,3

[a]ITS1 sequences are only alignable when gap costs are significantly reduced (Existence: 2, Extension: 2). ITS1 sequences in public repository records are typically flanked by short regions of 18S and 5.8S sequence.

tomes of bee BioSamples SAMN02870293 (cfr. *Apicystis bombi*) and SAMN07691958 (cfr. *Apicystis cryptica* sp. n.). The pairwise nucleotide identity between *A. bombi* and *A. cryptica* sp. n. transcripts ranged from 74.4% for rps6 to 82.7% for ef1a (mean 78.0%). The pairwise protein identity of translated open reading frames ranged from 81.25% for rps6 to 96.5% for ef1a (mean 90.2%).

Infection of the fat body and hypopharyngeal gland

The *B. pascuorum* female with a high *A. cryptica* sp. n. infection load (B05) was examined by light microscopy. Compared to the typical yellowish fat globules in a healthy individual B04, infected fat globules appeared swollen
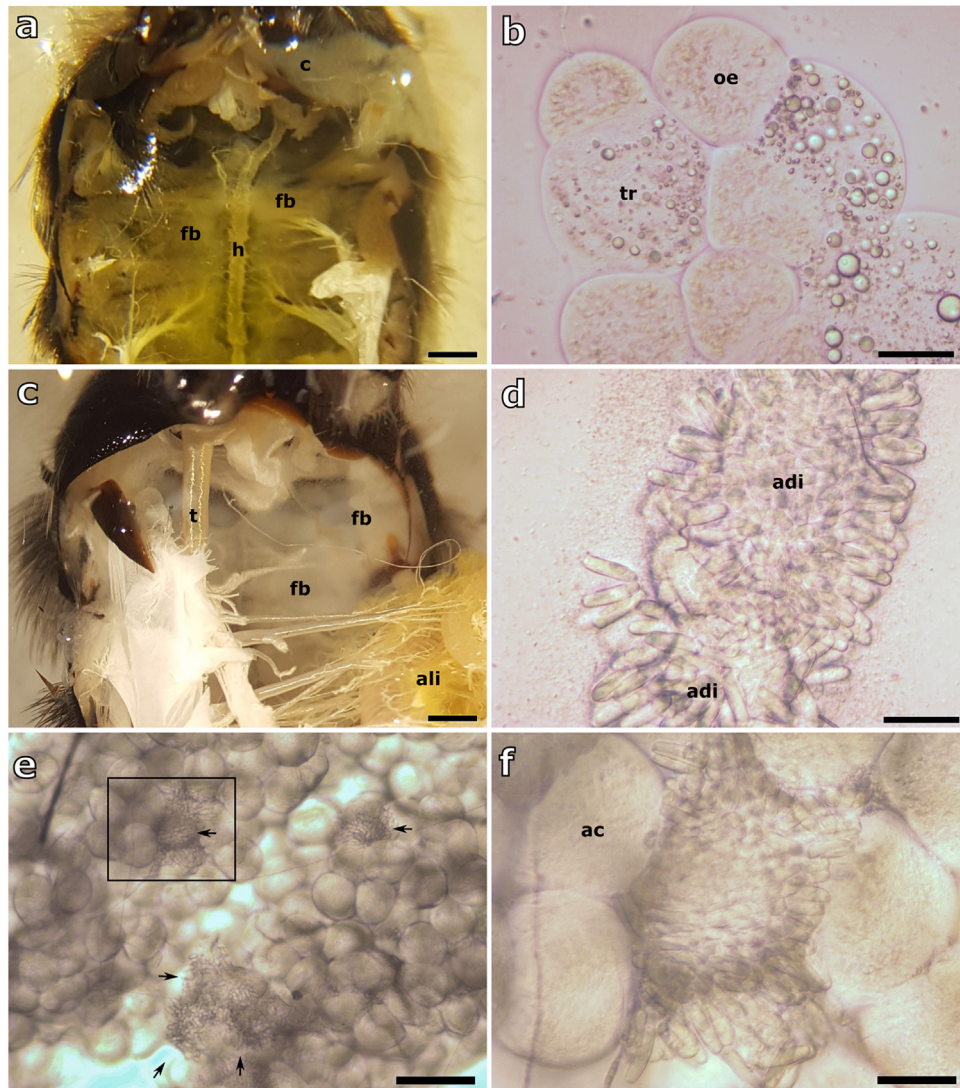
Fig. 3. a–f. Light microscopy of healthy and *Apicystis cryptica* sp. n. infected fat body and hypopharyngeal gland cells in a *Bombus pascuorum* female. **a)** Eviscerated metasoma of a healthy bumble bee. Sternites have been removed to visualize the interior side of the tergites. Parietal fat body is located as a uniform layer directly below the exoskeleton. Healthy fat body is coloured yellow. **b)** 400× magnification of a healthy fat body globule composed of the two adipocyte cell types: big-nucleated oenocytes and vacuolated trophocytes. **c)** Eviscerated metasoma of a diseased bumble bee. The parietal fat body is heavily infected and appears swollen and dully white instead of yellow. Note the bee heart is no longer visible between the parietal fat body layer. **d)** 400× magnification of hypertrophied fat body cells. Navicular oocysts are tightly packed inside a cell-like sphere. Oocysts are arrayed side-by-side near the cell periphery. Infected adipocytes are significantly enlarged. **e–f)** Oocyst-filled acini cells of the hypopharyngeal gland of the same infected bumble bee as in c and d. Infected acini (arrows) appeared randomly in between the cluster of healthy acini. ac, acini; adi, adipocyte; ali, alimentary tract; c, crop; fb, fat body; h, heart; oe, oenocyte; t, trachea; tr, trophocyte. Scale bars: a, c =1 mm; e = 100 μm; b, d, f = 25 μm. (For interpretation of the references to colour in this figure legend, the reader is referred to the web version of this article).

and white (Fig. 3a–c). Individual infected adipocytes were densely occupied by mature oocysts (Fig. 3d). The contours of the adipocytes were only distinguishable by means of the peripheral row of arrayed oocysts. All adipocytes were occupied by oocysts, indicating that both oenocyte and trophocyte cell types were infected. A similar hypertrophism was observed in a small number of HG cells (Fig. 3e): infected HG cells were also densely occupied by mature oocysts. However, the majority of HG cells appeared healthy, sug-

gesting that this tissue is not the primary infection target of *A. cryptica* sp. n. No oocysts or other developmental stages were observed in AL, MT, MU and OV tissues.

The ultrastructure of oocysts are comparable between species

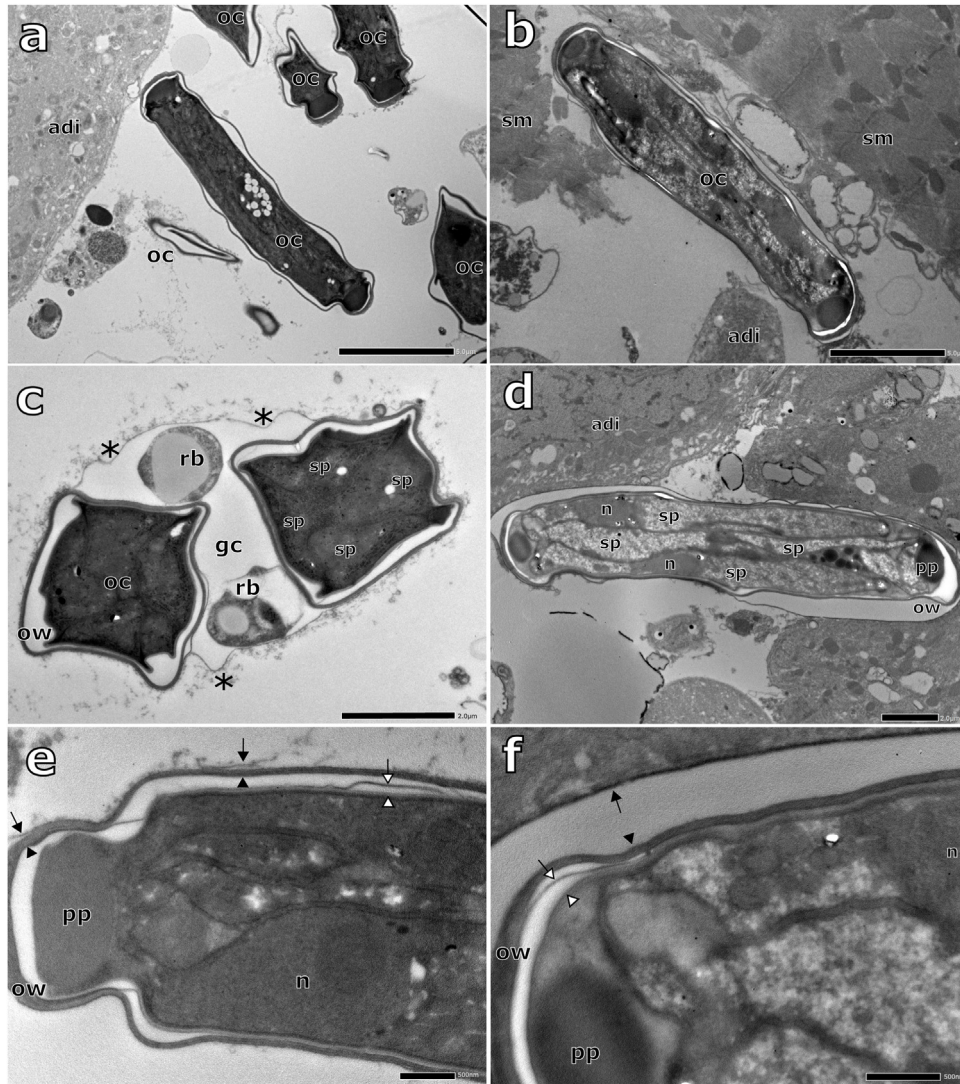Six tissue types of bumble bees infected with *A. bombi* (B06) and *A. cryptica* sp. n. (B10) were examined for the

Fig. 4. Transmission electron microscopy of *Apicystis bombi* and *Apicystis cryptica* sp. n. oocysts. *Apicystis bombi* in left-side micrographs and *A. cryptica* sp. n. in right-side micrographs from fat body tissue of *Bombus pascuorum* (respectively samples B06 and B10). **a)** Longitudinal section of a navicular oocyst of *A. bombi*. Other oocysts are visible adjacent to a healthy adipocyte cells. The oocysts have an electron-dense appearance. **b)** Longitudinal section of the navicular oocyst of *A. cryptica* sp. n. Oocysts were not observed in pairs and appeared less electron dense compared to maturing *A. bombi* oocysts. Next to healthy adipocytes, the fat body tissue also contained smooth muscle cells. **c)** Transverse section of two oocysts and two residual bodies associated in a gametocyst. The gametocyst membrane is readily visible (asterisks). Each oocyst contains four sporozoites that are enclosed by an electron-lucent oocyst wall of variable thickness. **d)** Longitudinal section of a mature *A. cryptica* sp. n. oocysts containing four sporozoites arranged side-by-side. The upper and lower sporozoites are complete and the electron-dense nuclei are distinctly stained. The two middle sporozoites are bend out of the visual plane and appear intertwined. The oval polar plugs at the oocyst poles stained dark. **e)** Close-up micrograph of an *A. bombi* oocyst pole with detailed bilayered composition of the oocyst wall. The inner bilayer consists of a thin external membrane (white arrow) and a broad internal membrane (white arrowhead) directly enclosing the sporozoites. The outer bilayer has a similar structure, consisting of a very thin external membrane (black arrows) and a broad internal membrane (black arrowheads). The broad internal membrane of the outer layer is averagely 70 nm thick and becomes thicker near the oocyst poles. The inner and outer bilayers are separated by an electron-lucent space. **f)** Close-up of *A. cryptica* sp. n. oocyst pole, showing the thickening of the oocyst wall between the internal (black arrowhead) and external (black arrow) membranes of the outer bilayer. The external membrane stains very dark. adi, adipocyte cells; gc, gametocyst; n, nucleus; oc, oocyst; ow, oocyst wall; pp, polar plug; rb, residual body; sm, smooth muscle cells; sp, sporozoite. Scale bars: a, b = 5 μm; c, d = 2 μm; e, f = 500 nm.

presence of oocysts or other developmental stages by TEM. Oocysts of both species were navicular in shape and contained four sporozoites (Fig. 4a, b). Oocysts were observed in FB tissue but were absent from HG, AL, MT, MU and OV

tissues. Oocysts of *A. bombi* were associated in pairs (Fig. 4c) but this was not observed for *A. cryptica* sp. n. Oocysts of the latter appeared less electron-dense with thicker walls indicating a more advanced stage of maturation. The structure of

the oocyst wall was comparable between the species despite the difference in maturation (Fig. 4e, f). For *A. bombi*, also non-synchronous transition of sporoblasts into young oocysts inside the gametocyst were observed (Supplemental Fig. 2). No free trophozoites were detected and no merogonial stages were found inside fat body cells or in the other tissues.

Mature oocysts of *A. cryptica* sp. n. in *B. pascuorum* are longer than oocysts of *A. bombi* in *B. terrestris*

Mature oocysts width and length were measured in fresh and TEM-fixed preparations. Oocyst sizes of historical reports and this study are summarized in Table 3. Fresh *A. bombi* mature oocysts measured 14.8 ± 0.8 μm $\times 4.5 \pm 0.2$ μm (A96 and A50, n = 47), the smallest oocyst was 13.2×4.1 μm and the largest oocyst was 16.4×4.8 μm. Fresh *A. cryptica* sp. n. mature oocysts measured 17.4 ± 0.8 μm $\times 5.3 \pm 0.2$ μm (A06 and A88, n = 51), min. 15.9×4.9 μm and max. 18.8×6.2 μm. Oocysts longer than 20 μm were not encountered. The fresh oocyst sizes were significantly different between species (Welch Two Sample t-test, $p < 0.05$, n = 98), although it should be noted that samples originated from different bumble bee host species. For both *A. bombi* and *A. cryptica* sp. n., a small number of angled oocysts were observed. Fixed *A. bombi* immature oocysts measured 13.7 ± 0.8 μm by 2.8 ± 0.2 μm (B06, n = 8), min. 12.4×2.7 μm and max. 14.9×2.9 μm. Fixed *A. cryptica* sp. n. mature oocysts measured 17.0 ± 0.9 μm $\times 3.7 \pm 0.5$ μm (B10, n = 3).

Discussion

In this study, a new gregarine species is described based on morphological and genetic data. We demonstrated that this parasite is able to infect the fat body cells of bumble bees and produces navicular oocysts containing four sporozoites. Together, these are the taxonomic descriptive features of the genus *Apicystis* which was monotypic until now. Comparison of ribosomal and protein-coding DNA sequences of the new gregarine to the respective DNA sequences of *Apicystis bombi* revealed that there is considerable divergence between the two (up to 31% nucleotide dissimilarity). Despite of this notable molecular divergence, oocyst morphology is highly comparable between the species. For the new species, we propose the name *Apicystis cryptica* sp. n. The delineations of *A. bombi* and *A. cryptica* sp. n. is in line with recent discoveries of cryptic bee parasite including *Crithidia mellificae* and *Lotmaria passim* (Schwarz et al. 2015), *C. bombi* and *C. expoeki* (Schmid-Hempel and Tognazzo 2010), and *Nosema apis* and *N. neumanii* (Chemurot et al. 2017). All of these delineation descriptions relied on molecular divergence by comparing sequence diversity across multiple loci.

Table 3. Comparison of *Apicystis* spp. oocyst sizes across different studies.

Study	Species[a]	Host species	Location	Oocyst size (μm)[b]	L:W[c]	Tissue
Liu et al. (1974)	Ap?	*Bombus* spp.	Canada, N-America	16.2×5.4 (young) / $21.6 - 27 \times 5.4$ (mature)	3.00 / 4.50	Fat body, midgut, hindgut, spermatheca
Lipa and Triggiani (1996)	Ap?	*Bombus* spp., *Apis mellifera*	Italy, Europe	$16.2 - 21.6 \times 5.6$	3.38	Fat body
Plischuk and Lange (2009)	Ap?	*B. terrestris*	Argentina, S-America	$12.94 \pm 0.08 \times 3.36 \pm 0.04$	3.85	Fat body
Plischuk et al. (2011)	ApB	*A. mellifera*	Argentina, S-America	$11.31 \pm 0.07 \times 3.21 \pm 0.03$	3.52	Fat body
Plischuk et al. (2011)	ApB	*B. terrestris*	Argentina, S-America	$12.94 \pm 0.08 \times 3.36 \pm 0.04$	3.85	Fat body
This study	ApB	*B. terrestris*	Belgium, Europe	$14.8 \pm 0.8 \times 4.5 \pm 0.2$ / $13.2 - 16.4 \times 4.1 - 6.2$	3.30	Fat body
This study	ApC	*B. pascuorum*	Belgium, Europe	$17.4 \pm 0.8 \times 5.3 \pm 0.2$ / $15.9 - 18.8 \times 4.9 - 6.2$	3.29	Fat body, hypopharyngeal gland

[a] Ap?, *Apicystis* sp.; ApB, *Apicystis bombi*; ApC, *Apicystis cryptica* sp. n.
[b] Measurement values are expressed as mean ± SEM or minimum-maximum, all values in μm. Unless indicated, sizes are of fresh (unfixed), mature oocysts.
[c] Length:Width ratio was obtained by dividing the mean length by the mean width.

The pathology of *A. bombi* and *A. cryptica* sp. n. predominantly takes place in the fat body tissue of the host. However, we observed a small number of acini cells of the prosomal HG tissue infected with *A. cryptica* sp. n. which is an uncommon tissue target for gregarines. Species in the related genera *Mattesia* and *Ophryocystis* mainly replicate in the FB and MT, respectively (Yaman and Radek 2017). Oocysts of one described *Mattesia* sp. accumulate in the prosoma of adult ants, but it is unclear if HG cells are targeted (Pereira et al. 2002). The few infected HG cells that we observed were likely associated with an advanced stage of infection. Most of the FB tissue was already hypertrophied by *A. cryptica* sp. n. hence the HG may serve as a secondary target tissue. Another explanation for this observation may involve the infection of HG cells as part of the parasite's transmission strategy. The HG is an excretory organ that is involved in the feeding of brood by young honey bee workers (Knecht and Kaatz 1990). Hence, oocysts that reach the HG duct through the infection of acini cells are passed on via glandular secretions to the progeny in the nest, a transmission strategy also reported for a picornavirus (Bailey 1969). The main transmission route of gregarines is considered by defecation and ingestion of contaminated food sources (oral-fecal transmission route) followed by sporozoite penetration of the intestinal epithelium. However, gregarines have also been reported in the reproductive system of insects (Dias et al. 2017) suggesting that some species have the potential to be transmitted during copulation (venereal transmission). Next to hypertrophies in the fat tissue, Liu et al. (1974) reported mature *A. bombi* oocysts in spermatheca of bumble bee queens. Whether *Apicystis* spp. oocysts are effectively passed on by glandular secretions or by venereal transmission awaits experimental confirmation.

A comprehensive investigation of developmental stages and life cycle morphological differences between *A. bombi* and *A. cryptica* sp. n. fell out of the scope of this study. However, we found gametocysts of *A. bombi* and confirmed the observations done by Liu et al. (1974) that sporoblasts develop in pairs inside the gametocyst membrane. The gametocyst stage was not found in *A. cryptica* sp. n. TEM analysis likely because the infection was too low. The fat body tissue is a large, scattered tissue and we might have missed the start point of infection which is considered to take place locally in a small subset of tissue. In order to observe potential life cycle differences between the species, standardized single infections as done by Graystock et al. (2016) are necessary to compare the developmental stages of the parasites.

A quick and reliable morphological marker would benefit pathogen monitoring studies that intend to discriminate *A. bombi* and *A. cryptica* sp. n. by light microscopy. However, the navicular shape of *A. bombi* oocysts was a characteristic feature that is now ambiguous. A potential morphological marker could be oocyst size, although evidence so far indicates that oocysts sizes are highly variable and influenced by maturation stage, geographical location and host species. Previous studies reported a size variation of up to 60% between young and mature oocysts (Lipa and Triggiani 1996; Liu et al. 1974; Plischuk and Lange 2009, summarized in Table 3). Also, Plischuk et al. (2011) reported validated *A. bombi* oocyst sizes in *B. terrestris* that were 13% smaller than *A. bombi* oocyst sizes in *B. terrestris* reported here. They also observed size differences in function of the host species with *A. bombi* oocysts being smaller in honey bees than in bumble bees. In the present study, *A. bombi* oocysts were obtained from *B. terrestris* individuals whereas *A. cryptica* sp. n. oocysts were obtained from *B. pascuorum* individuals. Although our measurements suggest that *A. cryptica* sp. n. oocysts are slightly longer than *A. bombi*, the size difference may be attributed to one or more of the above mentioned factors. Intraspecific size variability of *Apicystis* spp. thus appears common and may impede the use of oocyst size as a morphological marker.

The specific PCR assays that were designed in this study are currently the only scalable diagnostic tool for *A. bombi* and *A. cryptica* sp. n. However, the specificity of a pathogen detection assay only reaches as far as the hitherto knowledge of underlying species diversity. If more *Apicystis* species are discovered in the future (Fig. 2, at least one more *Apicystis* sp. is detected in transcriptome data of *Megachile willughbiella* in Germany (Peters et al. 2017, unpublished data)), it is likely that abandoning the 18S rDNA locus and replace it by one or more less conserved protein-coding genes, for example in Gisder and Genersch (2013), will be inevitable. A temporarily solution may rely in adopting more sensitive molecular methods such as high resolution melting (Higuera et al. 2013) or fragment length polymorphism (Ravoet et al. 2015). Alternatively, an efficient though costly method remains PCR amplification and Sanger sequencing of the ribosomal ITS1 region. The ITS1 sequence bears a high interspecific divergence and provides additional information about intraspecific haplotype structuring (Maharramov et al. 2013).

Taxonomic summary

Superphylum Alveolata Cavalier-Smith, 2010

Infraphylum Apicomplexa Levine, 1970

Class Gregarinomorphea Grassé, 1953

Order Arthrogregarida Cavalier-Smith, 2014

Superfamily Actinocephaloidea Léger, 1892

Family Lipotrophidae Grassé, 1953

Genus *Apicystis* Lipa and Triggiani, 1996

Species *Apicystis cryptica* sp. n.

Diagnosis. Molecular detection by PCR and specific primer pairs: forward ApC500f 5'-CAACCCCATGCAAGTATCAA and reversed ApC666r 5'-TGCCAATAAAAACAAAGCTCAA. GenBank accessions: 18S rDNA gene MF998086.1 and ITS1 sequence

KY126621. Oocysts navicular in shape and contain four sporozoites. Mature oocysts 17.4 ± 0.8 μm × 5.3 ± 0.2 μm in fresh extracts (minimal size 15.9 μm × 4.9 μm and maximal size 18.8 μm × 6.2 μm). Angled oocysts present but infrequent.

Etymology. The species-group name *cryptica* is derived from the English noun cryptic meaning secret, concealed. It refers to the morphological similarity to *A. bombi* and the need for molecular techniques in order to differentiate it from that species.

Hosts. The host of the *A. cryptica* sp. n. holotype is a female worker bee of *Bombus pascuorum*. The parasite was first detected in a metagenomic survey in wild-caught *B. pascuorum* queens in Belgium 2015 (Schoonvaere et al. 2018). Other host species where *A. cryptica* sp. n. has been detected are *B. sichelii* and *B. veteranus* from West-Siberia (GenBank records KY126625.1 and KY126621-2.1, respectively).

Infection Site. The primary infection site is the fat body tissue without discrimination between oenocyte and trophocyte cell types. *Apicystis cryptica* sp. n. can also infect acini cells of the hypopharyngeal gland tissue.

Type locality. The locality of the *A. cryptica* sp. n. holotype is Moorsel, East-Flanders, Belgium (50°57′12.5″N 4°06′28.9″E). The host bee was foraging on flowers of raspberry *Rubus fruticosus* upon capture.

Type material. Embedded Spurr resin of the holotype specimen of *A. cryptica* sp. n. in fat body tissue (accession number NeoFBs11) were deposited in the L-MEB collection, Ghent, Belgium. Next to the type material, embedded *Apicystis bombi* infected fat body tissue (accession numbers ApiBFBs2 and ApiBFBs6) are also available in this collection.

ZooBank registration. The new species was registered by LSID: urn:lsid:zoobank.org:act:92BE7D15-9F2A-4E38-936A-54DAFD527074.

Conclusion

A cryptic parasite species of bees is described based on morphological and molecular divergence evidence. The name *Apicystis cryptica* sp. n. is proposed and derives from its ambiguous oocyst morphology with respect to *Apicystis bombi*. Despite of similar morphology between both species, their molecular divergence is pronounced. Phylogeny based on the 18S rDNA gene confirmed the evolutionary relationship of both species. Interspecific nucleotide identity is as low as 69% for the ITS1 ribosomal sequence and on average 78% for seven protein-coding genes. We argue that the identification of *A. bombi* was systematically overestimated in previous studies for three reasons. First, *A. bombi* detection heavily relied on light microscopy and the presence of navicular oocysts in crude bee extracts or fat body tissue smears. It turns out that *A. cryptica* sp. n. oocysts have an identical navicular shape, making it impossible to discriminate the one from the other based on this feature. Second, the PCR primers used in more recently developed molecular detection assays were non-specific as they bound to a conserved region of the 18S rDNA gene. Hence, *A. cryptica* sp. n. was equally picked up by these assays implicating that all molecular identifications of *A. bombi* were overestimated. Third, preliminary insights suggest that the distribution and host occupation of *A. bombi* and *A. cryptica* sp. n. overlap. To date, both parasites have been found in *Bombus pascuorum* in Belgium and West-Siberia. Therefore, implementation of the specific PCR assays developed in this study will give a more accurate view on the prevalence, distribution and host specificity of *A. bombi* and *A. cryptica* sp. n.

Author contributions

DDG, MB and KS conceived the study. MB and KS carried out dissections of bumble bee tissues. KS carried out sampling, light microscopy and molecular work throughout the study. FB, MDB and RDR carried out preparations and imaging of the transmission electron microscopy analysis; KS, RDR and DDG interpreted the results. KS and DDG wrote the manuscript. All authors revised the manuscript and approved the final version of it.

Funding

CRediT authorship contribution statement

Karel Schoonvaere: Investigation, Visualization, Writing - original draft, Writing - review & editing. **Marleen Brunain:** Conceptualization, Methodology, Resources. **Femke Baeke:** Investigation, Resources. **Michiel De Bruyne:** Investigation, Resources. **Riet De Rycke:** Writing - original draft, Validation, Resources, Methodology. **Dirk C. de Graaf:** Supervision, Conceptualization, Validation.

Acknowledgements

expert reviewers for their helpful and constructive comments on the manuscript.

Appendix A. Supplementary data

Supplementary material related to this article can be found, in the online version, at doi:https://doi.org/10.1016/j.ejop.2020.125688.

References

Bailey, L., 1969. The multiplication and spread of sacbrood virus of bees. Ann. Appl. Biol. 63, 483–491, http://dx.doi.org/10.1111/j.1744-7348.1969.tb02844.x.

Cavalier-Smith, T., 2014. Gregarine site-heterogeneous 18S rDNA trees, revision of gregarine higher classification, and the evolutionary diversification of Sporozoa. Eur. J. Protistol. 50, 472–495, http://dx.doi.org/10.1016/j.ejop.2014.07.002.

Chemurot, M., De Smet, L., Brunain, M., De Rycke, R., de Graaf, D.C., 2017. Nosema neumanni n. sp. (Microsporidia, Nosematidae), a new microsporidian parasite of honeybees, Apis mellifera in Uganda. Eur. J. Protistol. 61, 13–19, http://dx.doi.org/10.1016/j.ejop.2017.07.002.

Dias, G., Dallai, R., Carapelli, A., Almeida, J.P.P., Campos, L.A.O., Faroni, L.R.A., Lino-Neto, J., 2017. First record of gregarines (Apicomplexa) in seminal vesicle of insect. Sci. Rep. 7, 1–9, http://dx.doi.org/10.1038/s41598-017-00289-3.

Gisder, S., Genersch, E., 2013. Molecular differentiation of Nosema apis and Nosema ceranae based on species–specific sequence differences in a protein coding gene. J. Invertebr. Pathol. 113, 1–6, http://dx.doi.org/10.1016/j.jip.2013.01.004.

Graystock, P., Goulson, D., Hughes, W.O.H., 2014. The relationship between managed bees and the prevalence of parasites in bumblebees. PeerJ 2014, 1–14, http://dx.doi.org/10.7717/peerj.522.

Graystock, P., Goulson, D., Hughes, W.O.H., 2015. Parasites in bloom: flowers aid dispersal and transmission of pollinator parasites within and between bee species. Proc. R. Soc. B Biol. Sci. 282, http://dx.doi.org/10.1098/rspb.2015.1371.

Graystock, P., Meeus, I., Smagghe, G., Goulson, D., Hughes, W.O.H., 2016. The effects of single and mixed infections of Apicystis bombi and deformed wing virus in Bombus terrestris. Parasitology 143, 358–365, http://dx.doi.org/10.1017/S0031182015001614.

Higuera, S.L., Guhl, F., Ramírez, J.D., 2013. Identification of Trypanosoma cruzi Discrete Typing Units (DTUs) through the implementation of a High-Resolution Melting (HRM) genotyping assay. Parasit. Vectors 6, 1–6, http://dx.doi.org/10.1186/1756-3305-6-112.

Jones, C.M., Brown, M.J.F., 2014. Parasites and genetic diversity in an invasive bumblebee. J. Anim. Ecol. 83, 1428–1440, http://dx.doi.org/10.1111/1365-2656.12235.

Knecht, D., Kaatz, H.H., 1990. Patterns of larval food production by hypopharyngeal glands in adult worker honey bees. Apidologie 21, 457–468, http://dx.doi.org/10.1051/apido:19900507.

Kumar, S., Stecher, G., Li, M., Knyaz, C., Tamura, K., 2018. MEGA X: molecular evolutionary genetics analysis across computing platforms. Mol. Biol. Evol. 35, 1547–1549, http://dx.doi.org/10.1093/molbev/msy096.

Lipa, J.J., Triggiani, O., 1992. A newly recorded neogregarine (Protozoa, Apicomplexa), parasite in honey bees (Apis mellifera) and bumble bees (Bombus spp). Apidologie 23, 533–536, http://dx.doi.org/10.1051/apido:19920605.

Lipa, J.J., Triggiani, O., 1996. Apicystis gen nov and Apicystis bombi (Liu, Macfarlane & Pengelly) comb nov (Protozoa: Neogregarinida), a cosmopolitan parasite of Bombus and Apis (Hymenoptera : Apidae). Apidologie 27, 29–34, Hal-00891321.

Liu, H.J., Macfarlane, R.P., Pengelly, D.H., 1974. Mattesia bombi n. sp. (Neogregarinida: Ophrocystidae), a parasite of Bombus (Hymenoptera: Apidae). J. Invertebr. Pathol. 23, 225–231, http://dx.doi.org/10.1016/0022-2011(74)90188-8.

Macfarlane, R.P., Lipa, J.J., Jiu, H.J., 1995. Bumble Bee Pathogens and Internal Enemies 76., pp. 130–148, http://dx.doi.org/10.1080/0005772X.1995.11099259.

Maharramov, J., Meeus, I., Maebe, K., Arbetman, M., Morales, C., Graystock, P., Hughes, W.O.H., Plischuk, S., Lange, C.E., De Graaf, D.C., Zapata, N., De La Rosa, J.J.P., Murray, T.E., Brown, M.J.F., Smagghe, G., 2013. Genetic variability of the neogregarine Apicystis bombi, an etiological agent of an emergent bumblebee disease. PLoS One 8, 6–13, http://dx.doi.org/10.1371/journal.pone.0081475.

Meeus, I., De Graaf, D.C., Jans, K., Smagghe, G., 2010. Multiplex PCR detection of slowly-evolving trypanosomatids and neogregarines in bumblebees using broad-range primers. J. Appl. Microbiol. 109, 107–115, http://dx.doi.org/10.1111/j.1365-2672.2009.04635.x.

Meeus, I., Brown, M.J.F., De Graaf, D.C., Smagghe, G., 2011. Effects of invasive parasites on bumble bee declines. Conserv. Biol. 25, 662–671, http://dx.doi.org/10.1111/j.1523-1739.2011.01707.x.

Menail, A.H., Piot, N., Meeus, I., Smagghe, G., Loucif-Ayad, W., 2016. Large pathogen screening reveals first report of Megaselia scalaris (Diptera: Phoridae) parasitizing Apis mellifera intermissa (Hymenoptera: Apidae. J. Invertebr. Pathol. 137, 33–37, http://dx.doi.org/10.1016/j.jip.2016.04.007.

Morimoto, T., Kojima, Y., Yoshiyama, M., Kimura, K., Yang, B., Peng, G., Kadowaki, T., 2013. Molecular detection of protozoan parasites infecting Apis mellifera colonies in Japan. Environ. Microbiol. Rep. 5, 74–77, http://dx.doi.org/10.1111/j.1758-2229.2012.00385.x.

Nunes-Silva, P., Piot, N., Meeus, I., Blochtein, B., Smagghe, G., 2016. Absence of Leishmaniinae and Nosematidae in stingless bees. Sci. Rep. 6, 2–6, http://dx.doi.org/10.1038/srep32547.

Pereira, R.M., Williams, D.F., Becnel, J.J., Oi, D.H., 2002. Yellow-head disease caused by a newly discovered Mattesia sp. in populations of the red imported fire ant, Solenopsis invicta. J. Invertebr. Pathol. 81, 45–48, http://dx.doi.org/10.1016/S0022-2011(02)00116-7.

Peters, R.S., Krogmann, L., Mayer, C., Donath, A., Gunkel, S., Meusemann, K., Kozlov, A., Podsiadlowski, L., Petersen, M., Lanfear, R., Diez, P.A., Heraty, J., Kjer, K.M., Klopfstein, S., Meier, R., Polidori, C., Schmitt, T., Liu, S., Zhou, X., Wappler, T., Rust, J., Misof, B., Niehuis, O., 2017. Evolutionary history of the Hymenoptera. Curr. Biol. 27, 1013–1018, http://dx.doi.org/10.1016/j.cub.2017.01.027.

Plischuk, S., Lange, C.E., 2009. Invasive Bombus terrestris (Hymenoptera: Apidae) parasitized by a flagellate (Euglenozoa: Kinetoplastea) and a neogregarine (Apicomplexa:

Neogregarinorida). J. Invertebr. Pathol. 102, 263–265, http://dx.doi.org/10.1016/j.jip.2009.08.005.

Plischuk, S., Meeus, I., Smagghe, G., Lange, C.E., 2011. *Apicystis bombi* (Apicomplexa: Neogregarinorida) parasitizing *Apis mellifera* and *Bombus terrestris* (Hymenoptera: Apidae) in Argentina. Environ. Microbiol. Rep. 3, 565–568, http://dx.doi.org/10.1111/j.1758-2229.2011.00261.x.

Plischuk, S., Antúnez, K., Haramboure, M., Minardi, G.M., Lange, C.E., 2017. Long-term prevalence of the protists *Crithidia bombi* and *Apicystis bombi* and detection of the microsporidium *Nosema bombi* in invasive bumble bees. Environ. Microbiol. Rep. 9, 169–173, http://dx.doi.org/10.1111/1758-2229.12520.

R Core Team, 2017. R: A Language and Environment for Statistical Computing. R Foundation for Statistical Computing, Vienna, Austria https://www.r-project.org/.

Ravoet, J., De Smet, L., Meeus, I., Smagghe, G., Wenseleers, T., de Graaf, D.C., 2014. Widespread occurrence of honey bee pathogens in solitary bees. J. Invertebr. Pathol. 122, 55–58, http://dx.doi.org/10.1016/j.jip.2014.08.007.

Ravoet, J., Schwarz, R.S., Descamps, T., Yañez, O., Tozkar, C.O., Martin-Hernandez, R., Bartolomé, C., De Smet, L., Higes, M., Wenseleers, T., Schmid-Hempel, R., Neumann, P., Kadowaki, T., Evans, J.D., de Graaf, D.C., 2015. Differential diagnosis of the honey bee trypanosomatids *Crithidia mellificae* and *Lotmaria passim*. J. Invertebr. Pathol. 130, 21–27, http://dx.doi.org/10.1016/j.jip.2015.06.007.

Rutrecht, S.T., Brown, M.J.F., 2008. The life-history impact and implications of multiple parasites for bumble bee queens. Int. J. Parasitol. 38, 799–808, http://dx.doi.org/10.1016/j.ijpara.2007.11.004.

Schmid-Hempel, P., 1998. Parasites in Social Insects. Princeton University Press.

Schmid-Hempel, R., Tognazzo, M., 2010. Molecular divergence defines two distinct lineages of *Crithidia bombi* (Trypanosomatidae), parasites of bumblebees. J. Eukaryot. Microbiol. 57, 337–345, http://dx.doi.org/10.1111/j.1550-7408.2010.00480.x.

Schoonvaere, K., De Smet, L., Smagghe, G., Vierstraete, A., Braeckman, B.P., De Graaf, D.C., 2016. Unbiased RNA shotgun metagenomics in social and solitary wild bees detects associations with eukaryote parasites and new viruses. PLoS One 11, http://dx.doi.org/10.1371/journal.pone.0168456.

Schoonvaere, K., Smagghe, G., Francis, F., de Graaf, D.C., 2018. Study of the metatranscriptome of eight social and solitary wild bee species reveals novel viruses and bee parasites. Front. Microbiol. 9, http://dx.doi.org/10.3389/fmicb.2018.00177.

Schulz, M., Ścibior, R., Grzybek, M., Łoś, A., Paleolog, J., Strachecka, A., 2019. A new case of honeybee *Apis mellifera* infection with bumblebee parasite *Apicystis bombi* (Apicomplexa: Neogregarinorida). Comp. Parasitol. 86, 65, http://dx.doi.org/10.1654/1525-2647-86.1.65.

Schwarz, R.S., Bauchan, G.R., Murphy, C.A., Ravoet, J., de Graaf, D.C., Evans, J.D., 2015. Characterization of two species of trypanosomatidae from the honey bee *Apis mellifera*: *Crithidia mellificae* Langridge and McGhee, and *Lotmaria passim* n. gen., n. sp. J. Eukaryot. Microbiol. 62, 567–583, http://dx.doi.org/10.1111/jeu.12209.

Stejskal, M., 1965. Gregarines parasitising honey bees. Am. Bee J. 105, 374–375.

Stucky, B.J., 2012. Seqtrace: a graphical tool for rapidly processing DNA sequencing chromatograms. J. Biomol. Tech. 23, 90–93, http://dx.doi.org/10.7171/jbt.12-2303-004.

Tamura, K., 1992. Estimation of the number of nucleotide substitutions when there are strong transition-transversion and G+C-content biases. Mol. Biol. Evol. 9, 678, http://dx.doi.org/10.1093/oxfordjournals.molbev.a040752.

Tian, T., Piot, N., Meeus, I., Smagghe, G., 2018. Infection with the multi-host micro-parasite *Apicystis bombi* (Apicomplexa: Neogregarinorida) decreases survival of the solitary bee *Osmia bicornis*. J. Invertebr. Pathol. 158, 43–45, http://dx.doi.org/10.1016/j.jip.2018.09.005.

Undeen, A.H., Vávra, J., 1997. Research methods for entomopathogenic Protozoa. Man. Tech. Insect Pathol., 117–151, http://dx.doi.org/10.1016/b978-012432555-5/50010-5.

Untergasser, A., Cutcutache, I., Koressaar, T., Ye, J., Faircloth, B.C., Remm, M., Rozen, S.G., 2012. Primer3-new capabilities and interfaces. Nucleic Acids Res. 40, http://dx.doi.org/10.1093/nar/gks596.

Valigurová, A., Koudela, B., 2006. Ultrastructural study of developmental stages of *Mattesia dispora* (Neogregarinorida: Lipotrophidae), a parasite of the flour moth *Ephestia kuehniella* (Lepidoptera). Eur. J. Protistol. 42, 313–323, http://dx.doi.org/10.1016/j.ejop.2006.07.007.

Yaman, M., Radek, R., 2017. *Ophryocystis anatoliensis* sp. nov., a new neogregarine pathogen of the chrysomelid beetle *Chrysomela populi*. Eur. J. Protistol. 59, 26–33, http://dx.doi.org/10.1016/j.ejop.2017.01.003.